

Effect of Closed Inelastic Channels on the Width of Resonances

JOSÉ R. FULCO*

Department of Physics, University of California, Santa Barbara, California

AND

GORDON L. SHAW†

Institute of Theoretical Physics, Department of Physics, Stanford University, Stanford, California

AND

DAVID Y. WONG‡

Department of Physics, University of California, San Diego, La Jolla, California

(Received 16 October 1964)

The effects of including nearby inelastic channels are examined on three separate examples of p -wave resonances: (a) a three-channel ($\pi\pi$, $\pi\omega$, $K\bar{K}$) system is treated in a calculation of the ρ (760 MeV) resonance, (b) a two-channel (πK , ηK) system is considered for the K^* (885) and, (c) a two-channel (πN , $K\Sigma$) system is treated for the N^* (1238). The input forces in (a) and (b) are taken to be due to the exchange of the known vector mesons and in (c) the baryons alone. The masses and coupling constants of the exchanged particles are taken from experiment; the coupling constants which cannot be related in a direct manner to experimental quantities are related to the others by the assumption of SU_3 symmetry. Straight cutoffs are used to insure that the multichannel ND^{-1} equations have a unique solution. Full numerical solutions of these equations are obtained by the matrix inversion technique. The values of the cutoffs were adjusted in the three examples to yield a peak in the cross section at the observed energy for the one-channel case and readjusted (to a lower value) to reproduce the resonant energy in the presence of the inelastic channels. This allows one to study the effect of the additional channels on the width and shape of the resonances. With the latter values of the cutoffs, the inelastic channels are turned off and the changes in the positions of the resonances are noted in order to estimate the relative contributions of the forces producing the resonance. It is noted, e.g., that the $\pi\omega$ channel has more effect on the position of the ρ than does the $K\bar{K}$ channel; also, the $K\Sigma$ channel has relatively little effect on the N^* (even though for pure SU_3 symmetry the N^* is equally composed of πN and $K\Sigma$). All the calculated widths are two to five times larger than the observed values, indicating that the lowest mass channels coupled via the longest range forces do not constitute a realistic model.

I. INTRODUCTION

ONE of the current problems in high-energy physics is the calculation of the properties of resonances by obtaining solutions of partial-wave dispersion relations. Since the input forces involve the exchange of these resonances themselves, the spin of some of them being ≥ 1 , some sort of high-energy cutoff is required in order to obtain solutions. Although one might, on physical grounds, put limits on the magnitude of the cutoff, the calculated positions of resonances are often quite sensitive to the exact value of the cutoff. One can only make it plausible that a particular resonant solution will result from a specific model of strong interactions. On the other hand, by adjusting the cutoff to produce a resonance at a given energy, one can make a theoretical prediction of the width.

In many of the relativistic calculations of resonances, the predicted widths are much broader than the observed widths. The statement is sometimes made that including nearby inelastic channels would greatly reduce this discrepancy.¹ The purpose of this article is

to examine this statement in a quantitative manner. We consider three separate examples of p -wave resonances which have been widely studied theoretically: ρ (760 MeV),^{2,3} K^* (885),⁴ and N^* (1238).⁵ The positions of these resonances are such that each can decay into only one channel. Most calculations ignore the closed inelastic channels and consider the resonances as one-channel systems. The results of these calculations all yield resonances which in addition to being too wide are (in contradiction with experiment) very asymmetric, i.e., the cross section falls off much slower on the high-energy side than on the low-energy side. By adding nearby inelastic channels in each case and solving the multichannel ND^{-1} equations we study, (i) the effect on the width, (ii) the effect on the shape, and (iii) the

narrow resonance will appear if the coupling to the open channel is arbitrarily weak.

² G. F. Chew and S. Mandelstam, *Nuovo Cimento* **19**, 752 (1961); J. S. Ball and D. Y. Wong, *Phys. Rev. Letters* **6**, 29 (1961); D. Y. Wong, *Phys. Rev.* **126**, 1220 (1962); L. A. P. Balázs, *ibid.* **129**, 872 (1963); **137**, B168 (1965).

³ F. Zachariasen and C. Zemach, *Phys. Rev.* **128**, 849 (1962). We refer to this paper as ZZ.

⁴ R. H. Capps, *Phys. Rev.* **131**, 1308 (1963); *Nuovo Cimento* **27**, 1208 (1963); *Phys. Rev. Letters* **10**, 312 (1963).

⁵ G. F. Chew and F. E. Low, *Phys. Rev.* **101**, 1570 (1956); W. R. Frazer and J. R. Fulco, *ibid.* **119**, 1420 (1960); S. Frautschi and J. Walecka, *ibid.* **120**, 1486 (1960); E. Abers and C. Zemach, *ibid.* **131**, 2305 (1962); J. S. Ball and D. Y. Wong, *ibid.* **133**, B179 (1964); A. Hendry and B. Stech, *ibid.* **133**, B191 (1964).

* Part of this work was done while the author (JRF) was at the University of California, San Diego.

† Supported in part by the U. S. Air Force through Air Force Office of Scientific Research Contract AF 49(638)-1389.

‡ Alfred P. Sloan Fellow.

¹ It is evident that if the forces in the closed channel alone are strong enough to produce a bound state, then an arbitrarily

relative contributions to the forces producing the resonance.

The program is the following: For each of the three above examples we compare single-channel calculations with multichannel calculations. The input forces are determined from single-particle exchange diagrams with the masses and coupling constants of the exchanged particles taken from experiment.⁶ SU_3 symmetry is assumed for the determination of those coupling constants which are not readily obtainable from experiments. A straight cutoff Λ is introduced to insure that the integral equations are of the regular Fredholm type and thus have a unique solution. For the one-channel calculation, Λ is adjusted to yield a peak in the output cross section corresponding to the experimental value. In all three examples, we find that the output width of the resonance is considerably larger than the experimental value. Also, unlike the observed shapes of the resonances which are approximately symmetric about the peak position, the calculated shapes are very asymmetric: the half-width at half-maximum on the high-energy side of the peak, Γ_H , is much larger than the corresponding value on the low-energy side Γ_L .⁷ Then an inelastic channel is added and Λ is readjusted (to a smaller value) to again reproduce the observed peak position. The effect of the inelastic channels on (i) the width and (ii) the shape of the resonance is

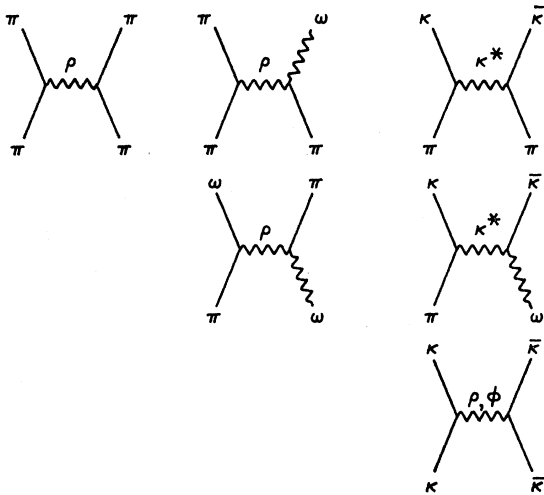


FIG. 1. Input forces in the three-channel calculation of the $\rho(760)$ resonance. The potential functions B_{ij} , Eqs. (8)-(13), are obtained by projecting out the $J=1$ partial-wave contributions from these diagrams. Channels 1, 2, and 3 correspond to $\pi\pi$, $\pi\omega$, and $K\bar{K}$, respectively.

⁶ We are interested in seeing how well the exchanges of the known particles reproduce themselves, in contrast with some calculations which are primarily concerned with finding a self-consistent (bootstrap) solution.

⁷ Note that for a wide resonance, the full width of the cross section is generally larger than that derived by taking the derivative of $\cot\delta$ and multiplying it by the phase-space factor evaluated at the zero of $\cot\delta$. In fact, the peak of cross section is also shifted significantly away from the zero of $\cot\delta$. The asymmetry of the resonance shape is due to these two effects.

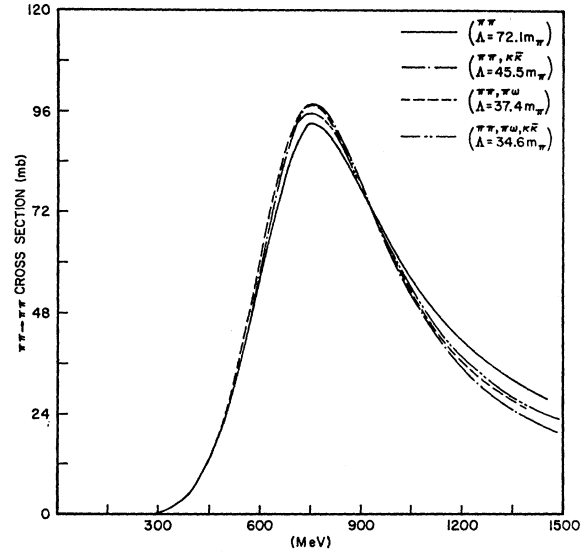


FIG. 2. Plots of the $I=1, J=1$ $\pi\pi$ cross section versus center-of-mass energy. The cutoff parameter Λ is separately adjusted for the one-, two-, and three-channel calculations of the ρ to reproduce the experimentally observed peak position. A narrowing of the calculated resonance by ≈ 100 MeV on the high-energy side is obtained in going from the one-channel calculation to any of the plotted multichannel calculations.

determined. Finally, with this latter value of Λ , the inelastic channels are turned off and the change in position of the resonance is noted in order to estimate (iii) the relative contribution of the forces producing the resonance. The same procedure may be repeated for additional inelastic channels.

The calculations for the ρ , K^* , and N^* are described in Secs. IIA, IIB, and IIC, respectively. Two inelastic channels were considered for the ρ resonance: $\pi\omega$ and $K\bar{K}$. Thus in addition to the one channel $\pi\pi$ calculation, two 2-channel calculations ($\pi\pi, \pi\omega$) and ($\pi\pi, K\bar{K}$) and a three-channel calculation ($\pi\pi, \pi\omega, K\bar{K}$) were performed. The input forces, shown in Fig. 1, were taken to be due to the exchange of the known vector particles. The $\rho\pi\pi$ and $\rho\pi\omega$ coupling constants are obtained from the experimental values of 100 and 9 MeV for the ρ and ω widths, respectively,⁸ and the remaining coupling constants are assumed to be related to these by SU_3 symmetry.⁹ We see, from Fig. 2 that the one-channel

⁸ *Proceedings of the International Conference on High Energy Physics, Dubna, 1964* (to be published).

⁹ M. Gell-Mann, *Phys. Rev.* **125**, 1067 (1962); California Institute of Technology Synchrotron Laboratory Report CTSL-20, 1961 (unpublished). The $K^*\pi K$ and $\phi K\bar{K}$ couplings can be obtained either from the $\rho\pi\pi$ coupling using SU_3 or from the experimental widths of 50 MeV for the K^* and 3 MeV for the ϕ . The two methods agree quite well. In spite of the fact that ϕ , K^* , and ρ do not satisfy the Gell-Mann-Okubo mass formula very well, it seems reasonable to treat them as members of an octet. The results of our calculation will not change significantly even if one takes a ω - ϕ mixing model of the singlet and the octet. We also note that a bootstrap model calculation of the vector octet [J. R. Fulco and D. Y. Wong, preceding paper *Phys. Rev.* **137**, B1239 (1965)] gives the splitting of the masses with the correct order of magnitude but the breaking of the coupling constant is $< 3\%$.

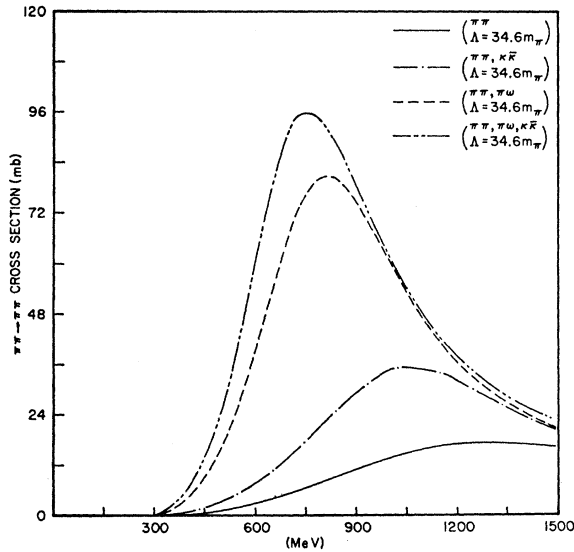


FIG. 3. The cutoff Λ is adjusted to give the observed position of the ρ peak for the three-channel calculation. Then the $\pi\omega$ and $K\bar{K}$ channels are switched off, keeping the same Λ , in order to determine the relative contribution of the forces producing the resonance. For example, we observe that the $\pi\omega$ channel has more effect on the position of the ρ than does the $K\bar{K}$ channel.

calculation requires a cutoff of $\Lambda = 72.1 m_\pi$ for $m_\rho = 760$ MeV and gives an output width $\Gamma = (\Gamma_H + \Gamma_L) \approx 600$ MeV with $\Gamma_L \approx 200$ and $\Gamma_H \approx 400$ MeV. For the same position of the ρ resonance, the $(\pi\pi, \pi\omega)$ problem requires $\Lambda = 37.4 m_\pi$ and for $(\pi\pi, K\bar{K})$, $\Lambda = 45.5 m_\pi$. Both two-channel calculations give a slightly smaller Γ_L whereas Γ_H is reduced to ≈ 300 MeV. The three-channel calculation requires $\Lambda = 34.6 m_\pi$ but the shape of the resonance is essentially the same as the two-channel ones. With a fixed cutoff $\Lambda = 34.6 m_\pi$, Fig. 3 indicates that the $\pi\omega$ channel contributes a substantial fraction of the force necessary to produce the ρ whereas the $K\bar{K}$ channel contributes relatively much less.

The diagrams corresponding to the forces in the K^* problem are given in Fig. 4. The cutoff for the one-channel (πK) calculation is $\Lambda = 219 m_\pi$ and the output width, as seen from Fig. 5, was ≈ 210 MeV with $\Gamma_L \approx 75$ MeV and $\Gamma_H \approx 135$ MeV. The two channel

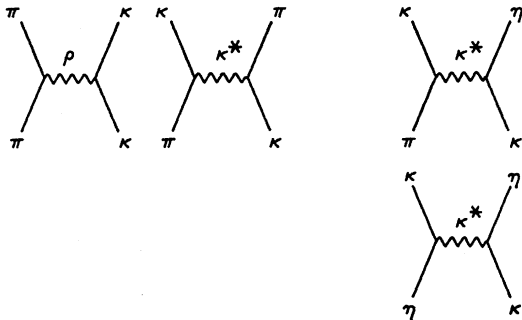


FIG. 4. Input forces in the calculation of the $K^*(885)$ resonance. Channel 1 corresponds to πK and channel 2 to ηK .

$(\pi K, \eta K)$ calculation required a cutoff of $\Lambda = 56.5 m_\pi$ and gave $\Gamma_L \approx 60$ MeV and $\Gamma_H \approx 95$. We note from Fig. 6 that the ηK channel plays a significant role in determining the position of the resonance.

In the $N^*(1238)$ calculation, Fig. 7, only baryon exchange was considered.¹⁰ We observe that the addition of the ΣK channel has a very small effect both on the width and position of the N^* . This (Figs. 8 and 9) may appear to be a little surprising since for unbroken SU_3 symmetry, the N^* is a 50-50 mixture of the two channels. However, the $K\Sigma$ threshold is substantially higher than that of πN and the cutoff required for the N^* problem is not very high (compared with the ρ and K^* cases). We have used a fixed cutoff in the total energy W , a fixed cutoff in the total kinetic energy, as well as a fixed cutoff in the total meson energy. In all three cases, the $K\Sigma$ contribution is so small that it can only shift the N^* position by $\lesssim 10$ MeV and has practically no effect on the width.

Our consistent failure to obtain sufficiently narrow resonance widths is rather disturbing. In particular, for

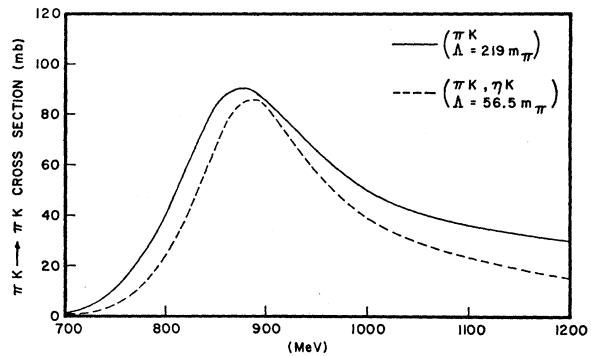


FIG. 5. Plots of the $I = \frac{1}{2}, J = 1$ πK cross section versus center-of-mass energy. Λ is separately adjusted for the one- and two-channel calculations of the K^* to reproduce the observed peak positions.

the case of the ρ resonance, even a three-channel calculation yields a full width which is approximately five times larger than the experimental value. However, since the two-channel $(\pi\pi, \pi\omega)$ calculation did narrow the calculated ρ width by 100 MeV as compared to the single-channel $\pi\pi$ calculation, we were led to examine a model in which the effect of the $\pi\omega$ channel was enhanced while the masses and input $\rho\pi\pi$ and $\rho\pi\omega$ coupling constants were still given by experiment. This was simply achieved by introducing different cutoffs in the two channels.¹¹ Two different approaches were considered: (1) a lower value of Λ was used for the $\pi\pi$ channel than the $\pi\omega$ channel; (2) an additional cutoff

¹⁰ The additional forces due to the exchange of the $N^*(1238)$ and ρ are rather weak in the $J = \frac{3}{2}, I = \frac{3}{2}$ amplitude; see Ref. 5.

¹¹ A single cutoff was used in the above calculations simply to reduce the number of parameters. Physically, it is not unreasonable for the cutoffs in different channels to be quite different. See, e.g., M. Bander and G. Shaw, Ann. Phys. (N. Y.) (to be published).

was introduced in the $\pi\pi$ channel on the left-hand cut (which thus diminished the force in the $\pi\pi$ channel due to ρ exchange) while the usual right-hand cutoff Λ was kept the same in both channels. For both approaches, the freedom of an additional parameter (a second cutoff) did not lead to any improvement over the results with a single cutoff. In fact, for cutoffs in the physical region of $\Lambda \approx 25 m_\pi$ for the $\pi\pi$ channel and $70 m_\pi$ for the $\pi\omega$ channel, the calculated width was as broad as the

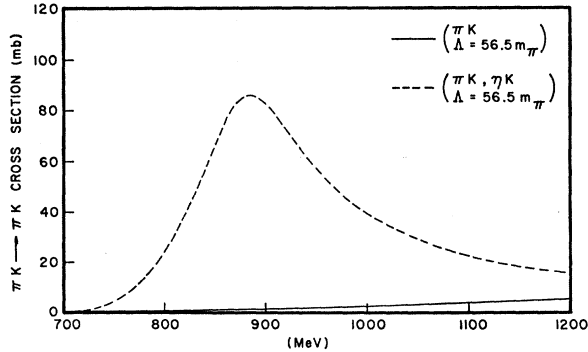
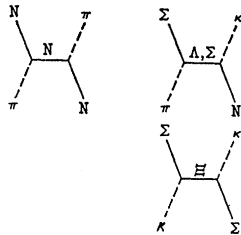


FIG. 6. The cutoff Λ is adjusted for the two-channel calculation to give the observed position of the K^* peak. A one-channel πK calculation with the same value of Λ is shown.

one-channel calculation. Physically, this is due to the fact that in this example, although the dominant force producing the ρ is in the $\pi\omega$ channel and the ρ appears as a "quasibound state," the coupling between the channels is also strong.¹ Thus we conclude that apparently, calculations of meson resonances (in particular, the ρ and K^*) including only the few lowest mass channels coupled via the longest range forces will not lead to agreement with experiment. One way of improving our model lies in a better treatment of the

FIG. 7. Input forces in the calculation of the $N^*(1238)$ resonance. Channel 1 corresponds to πN and channel 2 to $K\Sigma$.



asymptotic behavior of the amplitudes. It is rather likely that at extreme high energies, the amplitudes become pure imaginary because of increasing absorption. By just adding several nearby channels one will not obtain this result. A one-channel calculation of the ρ using an inelastic factor $(1-\eta)$ which starts off like the $\pi\pi-\pi\omega$ reaction but is allowed to stay large at high energy yields substantial improvement in the width.¹² A second point is that in our program of adding higher mass channels we did not change the left-hand singu-

¹² P. Coulter and G. Shaw (to be published).

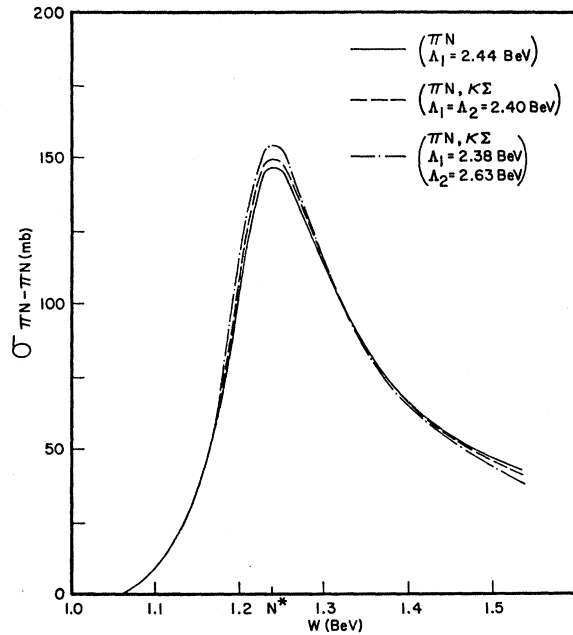


FIG. 8. Plots of the $I=\frac{3}{2}, J=\frac{3}{2} \pi N$ cross section versus center-of-mass energy W . Two different choices of cutoffs for the two-channel calculations are shown: same cutoff in W , and same cutoff on the meson energy. The cutoffs are separately adjusted for the one- and two-channel calculations of the N^* to reproduce the observed peak position.

larities in the elastic amplitude. Including the "continuum" contributions could make an improvement over our present results.

In spite of these possible modifications, it seems unlikely that they can change the calculated width by

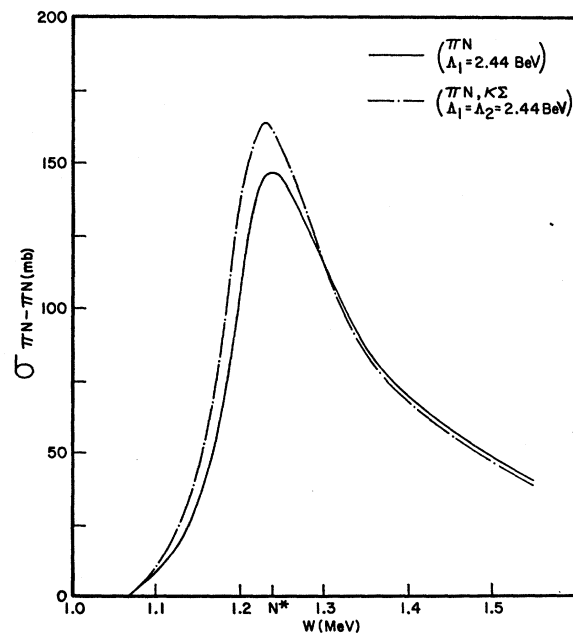


FIG. 9. The cutoff Λ_1 is adjusted for the one-channel calculation to give the observed position of the N^* peak. A two-channel calculation with the same value of $\Lambda_2 = \Lambda_1$ is shown.

a factor of 3 for the K^* and a factor of 5 for the ρ . On the other hand, one might argue that the cutoffs we employed here of the order 30–200 m_π are already so far into the higher energy region that other closed inelastic channels might be just as important. In particular, the baryon-antibaryon channels, having the property that they couple to the vector mesons in an S state, may be particularly favorable for producing the vector mesons as quasibound states. Furthermore, if Bronzan-Low's quantum number¹³ A is approximately preserved, one would expect that the coupling of the $N\bar{N}$ system to the two-pseudoscalar channels is sufficiently weak that the vector mesons will appear to be narrow resonances. Still another such possibility is that the $\pi\omega \rightarrow \pi\omega$ force could be largely due to the exchange of an $1^+ B$ meson which would enhance the attraction in the $\pi\omega \rightarrow \pi\omega$ amplitude. On the other hand, it does not directly couple to the $\pi\pi$ channel.¹⁴

As for the N^* , the discrepancy of the width between the static-theory calculation (which agrees with experiment) and the relativistic ND^{-1} results is also somewhat disturbing. However, the difference here is slightly less than a factor of 2, and the approximations made within the pseudoscalar-baryon model could possibly account for such discrepancies without recourse to additional channels.

Finally, we comment on the solution of the ND^{-1} equations. The numerical method we used was the matrix inversion technique for solving integral equations. The details are given in the Appendix. Two of the numerical checks of the program are the independence of the solution to the position of a subtraction in the D function and the symmetry of the T matrix as required by time reversal invariance. Many calculations have used the approximate solutions of the ND^{-1} equations given by the determinantal method which is quite sensitive to the value of the subtraction point. Also, straightforward application of the determinantal method violates time reversal invariance. For example, the two channel ($\pi\pi, \pi\omega$) calculation of the ρ by Zachariassen and Zemach³ (ZZ) leads to an amplitude $A_{\pi\pi \rightarrow \pi\omega}$ which is greatly different from $A_{\pi\omega \rightarrow \pi\pi}$. In addition, we note that the effect of the $\pi\omega$ channel was greatly enhanced in ZZ due to the fact that their ρ mass was 659 MeV, which is 121 MeV lower than the ω mass. Since the ω is almost unstable with respect to the $\pi\rho$ decay in their calculation, the ρ -exchange diagram for $\pi\omega \rightarrow \pi\omega$ contains a singularity very near the physical threshold, thus giving rise to an unrealistically strong force in that channel. In spite of this, their calculated width obtained via the derivative of the Breit-Wigner denominator is still approximately four times larger than the observed width.¹⁵ The width obtained by plotting the cross section is, as usual, even larger.

¹³ J. Bronzan and F. E. Low, Phys. Rev. Letters 12, 522 (1964).

¹⁴ J. Franklin (private communication).

¹⁵ There is a factor-of-4 error in the calculation of the ρ width in Ref. 3. The value of the calculated ρ width quoted there should be

II. MULTICHANNEL ND^{-1} EQUATIONS

A. The ρ Meson

The relativistically invariant matrix elements for the three-channel ($\pi\pi, \pi\omega, K\bar{K}$) partial-wave scattering amplitude, free from kinematical singularities and with the appropriate threshold behavior are defined by (we use units $\hbar=c=1$)

$$T_{ij}(s) = (\rho_i \rho_j)^{-1/2} t_{ij}, \quad i, j = 1, 2, 3, \quad (1)$$

where s is the square of the energy in the center-of-mass system and in the elastic region, $4m_\pi^2 < s < (m_\pi + m_\omega)^2$, $t_{11} = e^{i\delta_{\pi\pi}} \sin \delta_{\pi\pi}$.

The unitarity condition reads

$$\text{Im}[T_{ij}^{-1}(s)]_{ij} = -\delta_{ij} \theta(s - s_i) \theta(\Lambda_i - s) \rho_i(s) \quad (2)$$

where s_i and Λ_i are the threshold and the cutoff of the i th channel, respectively.

The phase space factors ρ_i are given by¹⁶

$$\rho_i = q_i^3 / \sqrt{s}, \quad i = 1 \text{ and } 3 \quad (3)$$

$$\rho_2 = q_2^3 \sqrt{s}, \quad (4)$$

where

$$q_1^2 = \frac{1}{4}s - m_\pi^2; \quad q_2^2 = [s - (m_\omega + m_\pi)^2][s - (m_\omega - m_\pi)^2]/4s;$$

and

$$q_3^2 = \frac{1}{4}s - m_K^2.$$

Using the ND^{-1} method and defining by $B_{ij}(s)$ the corresponding potentials (single-particle exchange amplitudes), we have¹⁷ for an n channel problem

$$T_{ij} = (ND^{-1})_{ij},$$

$$N_{ij}(s) = B_{ij}(s) + \sum_{k=1}^n \frac{1}{\pi} \int_{s_k}^{\Lambda_k^2} ds' K_{ik}(s, s') N_{kj}(s'), \quad (5)$$

that is, n systems of n coupled inhomogeneous integral equations for the matrix elements of N . The kernels are defined by

$$K_{ij}(s, s') = \left(\frac{1}{s' - s} \right) \left[B_{ij}(s') - \left(\frac{s - s_0}{s' - s_0} \right) B_{ij}(s) \right] \rho_i(s'). \quad (6)$$

The D_{ij} elements are given in terms of the N functions by

$$D_{ij}(s) = \delta_{ij} - \left(\frac{s - s_0}{\pi} \right) \int_{s_i}^{\Lambda_i^2} ds' \frac{\rho_i(s') N_{ij}(s')}{(s' - s_0)(s' - s)}. \quad (7)$$

multiplied by 4. See, for example, R. H. Capps, Phys. Rev. Letters 10, 312 (1963), footnote 6.

¹⁶ This form of the ρ functions can be readily seen from Eq. (2.21) of ZZ since the amplitudes t_{ij} defined there have kinematical singularities that can be eliminated by using the phase space factors (3), (4). This statement is however in disagreement with the paragraph preceding (2.11) of ZZ.

¹⁷ The following form of integral equations for the N functions was first published by J. Uretsky, Phys. Rev. 123, 1459 (1961).

It can be shown that the solutions of (5) and (7) are independent of the value of the subtraction point s , and T is symmetric (as required by invariance under time reversal) for a symmetric B .

In our calculation we limit ourselves to considering only the forces produced by the exchange of the known vector mesons. Then the potential functions $B_{ij}(s)$ are obtained by calculating the diagrams corresponding to Fig. 1. Following ZZ, the elements of the symmetric matrix $B_{ij}(s)$ are then given by¹⁸

$$B_{11}(s) = (g_{\rho\pi\pi}^2/4\pi)F_1(s, m_\pi, m_\pi, m_\rho), \quad (8)$$

$$B_{12}(s) = (g_{\rho\pi\pi}g_{\rho\pi\omega}/4\pi)F_2(s, m_\pi, m_\pi, m_\omega, m_\rho), \quad (9)$$

$$B_{13}(s) = (\frac{1}{2}\sqrt{8})(g_{K^*\pi K^2}/4\pi)F_1(s, m_\pi, m_K, m_{K^*}), \quad (10)$$

$$B_{22}(s) = (g_{\rho\pi\omega}^2/4\pi)F_3(s, m_\pi, m_\omega, m_\rho), \quad (11)$$

$$B_{23}(s) = (-\sqrt{\frac{2}{3}})(g_{K^*\pi K}g_{K^*K\omega}/4\pi)F_2(s, m_K, m_\pi, m_\omega, m_{K^*}), \quad (12)$$

$$B_{33}(s) = -\frac{1}{2}(g_{\rho K\bar{K}}^2/4\pi)F_1(s, m_K, m_K, m_\rho) + \frac{1}{2}(g_{\rho K\bar{K}}^2/4\pi)F_1(s, m_K, m_K, m_\varphi), \quad (13)$$

where

$$F_1(s, m_1, m_2, m) = (4/p^2q^2) \times [\frac{1}{2}m^2 + \frac{1}{2}s + (m_1^2 - m_2^2)^2/4m^2 - \frac{1}{2}(m_1^2 + m_2^2)]Q_1(Z), \quad (14)$$

$$Z = (m^2 + \frac{1}{2}s - m_1^2 - m_2^2)/(2pq), \quad (15)$$

$$F_2(s, m_1, m_2, m_3, m) = (\sqrt{2}/3pq)[Q_0(C) - Q_2(C)], \quad (16)$$

$$C = [m^2 + \frac{1}{2}(s + m_3^2 + m_2^2 + 2m_1^2)]/(2pq), \quad (17)$$

$$F_3(s, m_1, m_2, m) = (1/8sp^2) \times [\frac{1}{2}b_0 \ln((D+1)/(D-1)) + \bar{b}_0 - \frac{1}{3}p^2], \quad (18)$$

$$a_0 = p^2 + m_1^2, \quad a_1 = p^2 + s - (m_2^2 - m_1^2)^2/s, \quad (19)$$

$$a_2 = 3p^2 + 2m_2^2 + m_1^2, \quad a_3 = -p^2,$$

$$b_0 = a_0 - \bar{b}_0 D, \quad \bar{b}_0 = a_1 - a_2 D - a_3 D^2,$$

$$D = [s + 2(m^2 - m_1^2 - m_2^2) - (m_1^2 - m_2^2)^2/s]/(4p^2), \quad (20)$$

and where p and q are the momenta in the center-of-mass system of the initial and final particles, respectively.

By using the relations among the different coupling constants given by the unbroken eightfold way and

$$F(s, m_1, m_2, m_3, m_4, m) = \left(\frac{4}{p^2q^2}\right) \left[\frac{m^2}{4} + \frac{s}{2} + \frac{(m_1^2 - m_3^2)(m_2^2 - m_4^2)}{4m^2} - \frac{(m_1^2 + m_2^2 + m_3^2 + m_4^2)}{4} \right] Q_1(Z), \quad (28)$$

$$Z = [m^2 + \frac{1}{2}(s - m_1^2 - m_2^2 - m_3^2 - m_4^2) + (m_1^2 - m_2^2)(m_3^2 - m_4^2)/(2s)]/(2pq). \quad (29)$$

Again, by using the relations among the coupling constants given by the unbroken SU_3 , namely $g_{\rho\pi\pi}^2: g_{\rho K\bar{K}}^2: g_{K^*\pi K^2}: g_{K^*\eta K^2} = \frac{4}{3}: \frac{2}{3}: 1: 1$, we can compute all

¹⁸ There is apparently a printing error in Eq. (3.5) of ZZ where α should be replaced by β in the expressions for a_1 and a_2 .

assuming the ω to be a singlet,^{4,9} namely: $g_{\rho\pi\pi}^2: g_{\rho K\bar{K}}^2: g_{\rho K\bar{K}}^2: g_{K^*\pi K^2} = \frac{4}{3}: \frac{2}{3}: 2: 1$; $g_{\rho\pi\omega}^2 = g_{K^*\pi K^2}$, one can compute all the elements B_{ij} in terms of the $\rho\pi\pi$ and $\rho\pi\omega$ coupling constants. The values of these two parameters can be calculated from the experimental widths of the ρ and ω mesons. One obtains

$$(g_{\rho\pi\pi}^2/4\pi) = 0.45 \quad \text{for } \Gamma_\rho = 100 \text{ MeV}, \quad (21)$$

and

$$(g_{\rho\pi\omega}^2/4\pi) = 0.35 \quad \text{for } \Gamma_\omega = 9 \text{ MeV}. \quad (22)$$

We have then proceeded to solve Eqs. (5) and (7) for the one-channel ($\pi\pi$), two-channel ($\pi\pi, \pi\omega$) and ($\pi\pi, K\bar{K}$), and the three-channel ($\pi\pi, \pi\omega, K\bar{K}$) cases. First, by choosing different values of Λ to produce the resonance at the same position ρ (760), we were able to find out the effect of the higher mass channels on the width of the computed ρ meson. The results are reproduced in Fig. 2. Second, fixing the cutoff Λ in such a way as to produce a resonance at 760 MeV in the three-channel case, and using then the same value of Λ to solve the one-channel and both two-channel problems, we found the effect of the higher mass channels on the overall strength of the forces in the $J=1, I=1$ pion-pion amplitude. The results are shown in Fig. 3.

B. The K^* Meson

We consider the two-channel problem ($K\pi, K\eta$) and use the same formulation as for the ρ meson, except that now the phase space factors are given by

$$\rho_i(s) = q_i^3/\sqrt{s}; \quad i=1,2, \quad (23)$$

and

$$q_1^2 = [s - (m_\pi + m_K)^2][s - (m_\pi - m_K)^2]/(4s), \quad (24)$$

$$q_2^2 = [s - (m_\eta + m_K)^2][s - (m_\eta - m_K)^2]/(4s).$$

The input forces produced by the diagrams of Fig. 4 are now given by

$$B_{11}(s) = \sqrt{2}(g_{\rho\pi\pi}g_{\rho K\bar{K}}/4\pi)F(s, m_\pi, m_K, m_\pi, m_K, m_\rho) - \frac{1}{3}(g_{K^*\pi K^2}/4\pi)F(s, m_\pi, m_K, m_K, m_\pi, m_{K^*}), \quad (25)$$

$$B_{12}(s) = (g_{K^*\pi K}g_{K^*\eta K}/4\pi)F(s, m_\pi, m_K, m_K, m_\eta, m_{K^*}), \quad (26)$$

$$B_{22}(s) = (g_{K^*\eta K^2}/4\pi)F(s, m_\eta, m_K, m_K, m_\eta, m_{K^*}), \quad (27)$$

where

the elements $B_{ij}(s)$ in terms of the $\rho\pi\pi$ coupling constant [Eq. (21)].

As explained in Sec. IIA, we have first solved the one-channel and two-channel cases with different values of Λ to reproduce the resonance at the same energy K^* (885), and we have then looked at the effect of the

$K\eta$ channel in the width of the computed K^* . Fig. 5 shows the cross section obtained in this case. Secondly, we have investigated the effect of the higher mass channel on the position of the K^* by fixing the cutoff in the two-channel problem to obtain the resonance at 885 MeV and then using the same value of Λ in solving the one-channel case.

C. The N^* Resonance

It is well known that for the scattering of pseudo-scalar mesons from baryons it is more convenient to define the partial wave amplitudes as functions of the total energy W .⁵ We then choose the elements of the 2×2 scattering matrix for the πN and $K\Sigma$ $I = \frac{3}{2}$, $J = \frac{3}{2}$ state as^{5,19}

$$T_{ij}(W) = (2s)^2 (q_i q_j)^{-3/2} \left\{ [(W + m_i)^2 - \mu_i^2] \times [(W + m_j)^2 - \mu_j^2] \right\}^{-1/2} t_{ij}, \quad (30)$$

where again in the the elastic region $t_{11} = e^{i\delta_{\pi N}} \sin \delta_{\pi N}$.

The unitarity condition reads

$$\text{Im}[T^{-1}(W)]_{ij} = -\delta_{ij} \theta(s - s_i) \theta(\Lambda_i^2 - s) \rho_i(W), \quad (31)$$

where

$$\rho_i(W) = q_i^3 [(W + m_i)^2 - \mu_i^2] / (2s^2); \quad i = 1, 2 \quad (32)$$

$$q_i^2 = [s - (m_i + \mu_i)^2][s - (m_i - \mu_i)^2] / (4s), \quad (33)$$

and m_1, m_2, μ_1, μ_2 are the masses of the nucleon, Σ , π meson, and K meson, respectively.

Using the ND^{-1} method as before, one obtains

$$T_{ij}(W) = (ND^{-1})_{ij},$$

$$N_{ij}(W) = B_{ij}(W) + \sum_k \frac{1}{\pi} \int_{m_i + \mu_i}^{\Lambda_i} + \int_{-\Lambda_i}^{-m_i - \mu_i} dW' \times K_{ik}(W, W') N_{kj}(W'), \quad (34)$$

$$K_{ij}(W, W') = \left[B_{ij}(W') - \left(\frac{W - W_0}{W' - W_0} \right) B_{ij}(W) \right] \times \rho_i(W') / (W' - W). \quad (35)$$

Finally,

$$D_{ij}(W) = \delta_{ij} - \left(\frac{W - W_0}{\pi} \right) \times \int_{m_i + \mu_i}^{\Lambda_i} + \int_{-\Lambda_i}^{-m_i - \mu_i} dW' \frac{\rho_i(W') N_{ij}(W')}{(W' - W)(W' - W_0)}. \quad (36)$$

Here also the solutions to Eqs. (34) and (36) are independent of W_0 .

In the approximation which considers only the forces produced by the exchange of baryons, we have the diagrams shown in Fig. 7. The matrix elements of the potential are now given by

$$B_{11}(W) = 2(g_{\pi N^2}/4\pi)G(W, m_1, \mu_1, m_1, \mu_1, m_N), \quad (37)$$

$$B_{12}(W) = (g_{\Lambda\pi\Sigma}g_{\Lambda KN}/4\pi)G(W, m_1, \mu_1, m_2, \mu_2, m_\Lambda) - (g_{\Sigma\pi\Sigma}g_{\Sigma KN}/4\pi)G(W, m_1, \mu_1, m_2, \mu_2, m_\Sigma), \quad (38)$$

$$B_{22}(W) = 2(g_{\Sigma K\Sigma^2}/4\pi)G(W, m_2, \mu_2, m_2, \mu_2, m_\Sigma), \quad (39)$$

where the indices 1 and 2 refer to $N\pi$ and ΣK , respectively, and

$$G(W, m_i, \mu_i, m_j, \mu_j, m) = \frac{s}{4q_i^2 q_j^2} \left\{ (W - m_1 - m_2 + m) Q_1(Z) - [(W - m_1)^2 - \mu_1^2] \times [(W - m_2)^2 - \mu_2^2] \left(\frac{W + m_1 + m_2 - m}{4s q_i q_j} \right) Q_2(Z) \right\}; \quad (40)$$

$$Z = [s^2 - s(m_1^2 + m_2^2 + \mu_1^2 + \mu_2^2 - 2m^2) - (m_1^2 - \mu_1^2)(m_2^2 - \mu_2^2)] / 4q_i q_j s.$$

Within the approximation of the unbroken eightfold way, we have the following relations among the coupling constants¹⁹:

$$\begin{aligned} g_{\Lambda\pi\Sigma} &= (2/\sqrt{3})(1-f)g_{\pi N}, \\ g_{\Lambda KN} &= -(1/\sqrt{3})(1+2f)g_{\pi N}, \\ g_{\Sigma\pi\Sigma} &= 2fg_{\pi N}, \\ g_{\Sigma KN} &= (1-2f)g_{\pi N}, \\ g_{\Sigma K\Sigma} &= -g_{\pi N}, \end{aligned} \quad (41)$$

where

$$(g_{\pi N^2}/4\pi) \approx 14,$$

and f is the D/F branching ratio as defined in Ref. 19. It is difficult to estimate the degree of accuracy of Eqs. (41) since experimental values are not available for these coupling constants. There is also an ambiguity in the choice of the value of f , since one can follow several criteria to determine it and obtain different values in each case. One can ask for the value that produces the maximum strength of the forces in the $PS_8 + B_8 \rightarrow B_{10}$ interaction, as is done in Ref. 19 or use the idea of the conditions for a reciprocal bootstrap between the B_8 and B_{10} multiplets, as in the work of Cutkowsky²⁰ and Hara.²¹ In the first case one obtains $f \simeq 0.25$ and in the second $f \simeq 0.33$. Fortunately, these two values of f practically do not change the results of our model. We then use $f = 0.31$ and proceed as before by first fixing Λ_i to obtain the N^* at the same position (1238 MeV) in both the one-channel and two-channel cases. The effect of the $K\Sigma$ channel on the width of the computed N^* is shown in Fig. 8. Since the value of Λ_1 is not very far above the $K\Sigma$ threshold we have used three different criteria to select both cutoffs. First: $\Lambda_1 = \Lambda_2$ at the same total energy W . Second: by requiring the same cutoff on the total kinetic energy in each channel. Third: by using the same cutoff on the meson total energy. We have found that there is practically no difference among

¹⁹ A. W. Martin and K. C. Wali, Phys. Rev. **130**, 2455 (1963); Nuovo Cimento **31**, 1324 (1964).

²⁰ R. Cutkowsky, Ann. Phys. (N. Y.) **23**, 415 (1963).

²¹ Y. Hara, Phys. Rev. **135**, B1079 (1964).

the results obtained with the different choices of Λ_i . Then we adjust Λ_1 for the one-channel calculation to give the observed position of the N^* peak. A two-channel calculation with the same value of $\Lambda_2 = \Lambda_1$ is performed; Fig. 9 shows the results.

APPENDIX: NUMERICAL METHODS FOR SOLVING MULTICHANNEL ND^{-1} EQUATIONS

Once the potentials $B_{ij}(s)$ are given, the N functions can be calculated by solving the following Fredholm integral equations of the second kind:

$$N_{ij}(s) = B_{ij}(s) + \frac{1}{\pi} \int_{s_i}^{\Lambda_i^2} ds' \left(\frac{1}{s' - s} \right) \times \left[B_{ik}(s') - \left(\frac{s - s_0}{s' - s_0} \right) B(s)_{ik} \right] \rho_k(s') N_{kj}(s'), \quad (\text{A1})$$

where s_0 is the subtraction point for the D functions, s_i and Λ_i are the threshold and the cutoff, respectively, for the i th channel, and the ρ 's are the phase-space factors.

To solve Eq. (A1) by numerical methods, one would first replace the s' integration by a sum over a discrete set of values of s' . Using now superscripts for the channel indices and subscripts for the energy indices, we can write

$$N_k^{(i,j)} = B_k^{(i,j)} + \sum_{l,m} K_{kl}^{(i,m)} N_l^{(m,j)}, \quad (\text{A2})$$

where

$$K_{kl}^{(i,m)} = \frac{1}{\pi} (\Delta s)_l \left(\frac{1}{s_l - s_k} \right) \times \left[B_l^{(i,m)} - \left(\frac{s_k - s_0}{s_l - s_0} \right) B_k^{(i,m)} \right] \rho_l^{(m)}, \quad (\text{A3})$$

and $(\Delta s)_l$ is the mesh size for the l th value of s' . It is important that the mesh distribution be chosen appropriate to the rate of variation of the remaining factors of (A3). For $l = k$, the derivative of B with respect to s is required.

For any fixed index j , Eq. (A2) can be converted into a simpler matrix equation by combining the remaining channel indices and the energy indices. One obtains

$$\eta_\gamma^{(j)} = \beta_\gamma^{(j)} + \kappa_\gamma \delta \eta_\delta^{(j)}, \quad (\text{A4})$$

where

$$\eta^{(j)} = \begin{pmatrix} N_{m_1}^{(1,j)} \\ \vdots \\ N_{n_1}^{(1,j)} \\ N_{m_2}^{(2,j)} \\ \vdots \\ N_{n_2}^{(2,j)} \\ \vdots \end{pmatrix}, \quad (\text{A5})$$

$$\kappa = \begin{pmatrix} K_{m_1 m_1}^{(1,1)} \cdots K_{m_1 n_1}^{(1,1)} & K_{m_1 m_2}^{(1,2)} \cdots K_{m_1 n_2}^{(1,2)} & \cdots \\ \vdots & \vdots & \vdots \\ K_{n_1 m_1}^{(1,1)} \cdots K_{n_1 n_1}^{(1,1)} & K_{n_1 m_2}^{(1,2)} \cdots K_{n_1 n_2}^{(1,2)} & \cdots \\ \vdots & \vdots & \vdots \\ K_{m_2 m_1}^{(2,1)} \cdots K_{m_2 n_1}^{(2,1)} & K_{m_2 m_2}^{(2,2)} \cdots K_{m_2 n_2}^{(2,2)} & \cdots \\ \vdots & \vdots & \vdots \\ K_{n_2 m_1}^{(2,1)} \cdots K_{n_2 n_1}^{(2,1)} & K_{n_2 m_2}^{(2,2)} \cdots K_{n_2 n_2}^{(2,2)} & \cdots \\ \vdots & \vdots & \vdots \end{pmatrix}. \quad (\text{A6})$$

The indices m_i and n_i are energy indices corresponding to the threshold and the cutoff for the i th channel. The dimension of κ is equal to the sum

$$d_\kappa = \sum_{i=1}^n (n_i - m_i) \quad (\text{A7})$$

for an n -channel problem.

Now the solution of η , and hence the N functions, can be obtained by inverting the matrix in (A4)

$$\eta^{(j)} = (I - \kappa)^{-1} \beta^{(j)}. \quad (\text{A8})$$

Since the κ matrix is independent of the index j , only one matrix inversion is required. A standard subroutine called MATINV (SHARE as well as CDC) can be used to obtain $\eta^{(j)}$ for all j . The basic restriction of the numerical program is the limitation on the dimension d_κ which for practical purposes, should not exceed ≈ 100 . If one uses 20 mesh points for the lowest channel and successively fewer mesh points for higher channels, one could easily accommodate six or seven channels in the calculation.

For the three-channel problem of the ρ meson, sufficient accuracy is obtained with 20 mesh points for the $\pi\pi$ channel and 10 to 15 mesh points for $\pi\omega$ and $K\bar{K}$. The CDC 3600 will yield the solution for the three-channel η in the order of 15 seconds.

Having obtained the N function, one can calculate the D functions by evaluating the principal part integrals

$$\text{Re}(D_{ij}) = \delta_{ij} - \frac{s - s_0}{\pi} P \int_{s_i}^{\Lambda_i^2} ds' \frac{\rho_i(s') N_{ij}(s')}{(s' - s_0)(s' - s)}. \quad (\text{A9})$$

Usually, the time required to calculate D_{ij} is small compared to the matrix inversion program.

Aside from examining the stability of the numerical results with variation of mesh size, two checks of the numerical accuracy can be obtained by showing that, (i) the solution ND^{-1} is independent of the subtraction constant s_0 and, (ii) ND^{-1} is a symmetric matrix.